Theor Chem Acc (1997) 96:157–165

Theoretical
Chemistry Accounts

The vibrational spectra of the boron halides and their molecular complexes, part 5*

An ab initio study of the infrared spectrum of the boron trifluoride-carbon dioxide complex

L.M. Nxumalo[1], G.A. Yeo[2], T.A. Ford[3]

[1] Department of Chemistry, Vista University, Soweto Campus, Private Bag X09, Bertsham 2013, South Africa
[2] School of Chemistry, Technikon Witwatersrand, P.O. Box 17011, Doornfontein 2028, South Africa
[3] Centre for Theoretical and Computational Chemistry, Department of Chemistry and Applied Chemistry, University of Natal, Durban 4041, South Africa

Received: 18 November 1996 / Accepted: 11 March 1997

Abstract. The optimized structures, interaction energies, Mulliken charges and vibrational spectra of three conformers of a 1:1 complex between boron trifluoride and carbon dioxide have been determined by means of ab initio calculations at the second-order level of Møller-Plesset perturbation theory, using the 6-31G* basis set. All three structures feature a B···O electron donor-acceptor interaction. One of the structures, in which the carbon dioxide axis eclipses one of the BF bonds, was found to be a genuine minimum, one (the corresponding staggered form) a first-order saddle point and the third (a linearly bonded B···OCO species) a second-order transition state. The computed infrared spectrum of the preferred conformer has been used to predict the appearance of the spectrum of boron trifluoride and carbon dioxide co-deposited in cryogenic matrices, which will be reported in a forthcoming publication.

Key words: Vibrational spectra – Boron trifluoride – Carbon dioxide complexes

1 Introduction

In our recent ab initio studies of some binary Lewis acid-base complexes of boron trifluoride with some oxygen [1, 2], nitrogen [3–5], sulphur [2], fluorine [6] and carbon [7] bases, we have observed that these complexes display a wide range of structural, electronic, energetic and vibrational properties. In particular, the ways in which the vibrational spectrum of boron trifluoride is perturbed as a result of complexation with such bases may be correlated with the physical properties of the bases. Table A-1 reports the results of the calculations of the B···X intermonomer separation (X is the electronegative atom of the base, viz. O, N, S, F or C), the FB···X bond angle, the interaction energy and the B···X intermolecular stretching wavenumber of the aggregates of BF_3 with H_2O, $(CH_3)_2O$, N_2, HCN, FCN, C_2N_2, HC_3N, NH_3, NF_3, $(CH_3)_2S$, BF_3 and CO [1–8]. (Tables designated by a preceding A may be found in the internet archive [9].) For bases of the same type, the shorter B···X bond distances, larger FB···X bond angles and higher B···X bond stretching wavenumbers are associated with the higher interaction energies. References [3] and [7] contain a large number of citations of earlier work dealing with experimental and theoretical studies of boron trifluoride complexes. In every case, the electron donor-acceptor (EDA) interaction occurs between one of the lone-pair orbitals of the base and the molecular orbital of BF_3 dominated by the a_1 2*p* atomic orbital of the boron atom.

Carbon dioxide is known to form molecular complexes in the gas phase which may be of several types. Examples of such aggregates, detected in most cases by means of microwave, infrared or molecular beam electric resonance spectroscopy, include linear hydrogen-bonded complexes with acids like hydrogen fluoride [10–16], hydrogen chloride [14, 17] and hydrogen cyanide [18, 19]; T-shaped complexes with electron donors such as helium [20], neon [21–24], argon [21–23, 25–29], krypton [21, 22, 24], xenon [21, 24], mercury [30], nitrogen [31], hydrogen bromide [14, 32], deuterium bromide [33], carbon monoxide [34, 35], hydrogen cyanide [19, 36, 37], carbon dioxide [38–40], water [41, 42], hydrogen sulphide [43] and ammonia [44, 45]; and parallel complexes with carbon dioxide [23, 46–50], carbonyl sulphide [51], acetylene [52–54], formaldehyde [55] and ethylene [56].

*This article is supplemented by an internet archive which can be obtained electronically from the Springer-Verlag server located at http://link.springer.de/journals/tca/

Correspondence to: T. A. Ford
e-mail: ford@che.und.ac.za

Particularly noteworthy among this set of complexes are those between carbon dioxide and hydrogen cyanide, for which evidence exists for both a linear [18,19] and a T-shaped structure (19, 36, 37], depending on the carrier gas used in the experiments, and the carbon dioxide dimer. Early studies on carbon dioxide-hydrogen cyanide complexes [38–40] indicated a T-shaped structure, although more recent experiments [22, 45–49] favoured a slipped parallel orientation of the monomer units. The formaldehyde and ethylene complexes are also interesting cases. While $H_2CO{\cdot}CO_2$ is described as a parallel structure [55], this description refers to the alignment of the respective CO_2 and CO axes only; the structure is in fact a planar five-membered cyclic one, with electron donation occurring between the H_2CO oxygen and the CO_2 carbon atom, and between one of the CO_2 oxygen atoms and one of the H_2CO hydrogens. In the case of the ethylene adduct, while the CO_2 and CC axes are formally parallel, free internal rotation is observed to take place about the line joining the monomer centres of mass [56].

The vibrational spectra of several of these complexes have been recorded in cryogenic matrices including, among the linear complexes, those with hydrogen fluoride [57, 58] and hydrogen chloride [59, 60]. The complexes with carbon monoxide [61], water [62], ammonia [63] and formaldehyde [64] are T-shaped, and the original matrix isolation study of the carbon dioxide dimer [65] concluded that it, too, was T-shaped; later spectroscopic studies [66–69], however, came out in favour of a slipped parallel structure. An interesting example is provided by the spectrum of the complex between carbon dioxide and monatomic aluminium [70]; two structures were observed, a four-membered cyclic arrangement of C_{2V} symmetry and a planar trans Al—O—C=O species belonging to the C_S point group.

Of the large number of ab initio studies which have been undertaken, most provide qualitative confirmation of the experimental structures. The linear aggregates include the complexes with hydrogen fluoride [71–75], hydrogen chloride [71, 75, 76], hydrogen cyanide [19, 72, 77, 78], water [42, 72, 79–82] and acetylene [83, 84]. The complexes found to be T-shaped are those with helium [20, 85–88], neon [86], argon [26, 85, 89–91], hydrogen fluoride [71], hydrogen bromide [75], deuterium bromide [33], hydrogen cyanide [19, 36, 77, 78, 92], water [42, 71, 72, 79–82, 93, 94], hydrogen sulphide [71], acetylene [84], ammonia [71, 95, 96] and phosphine [71]. The carbon dioxide dimer was originally reported to be T-shaped [84, 97, 98], but the consensus of later publications [69, 84, 92, 98–105] agrees with the more recent experimental conclusions that it has the slipped parallel configuration. Other parallel carbon dioxide complexes reported are those with hydrogen cyanide [19], acetylene [83, 84, 103] and ethylene [56]. In many cases the investigators considered several possible structures [19, 42, 71, 72, 77–82, 84, 93, 98], and were able to identify the most and least probable alternatives.

The most interesting feature of these structural observations is that in the complexes of CO_2 with HF and HCl, the acid donates a proton along the molecular axis of the CO_2 molecule, while in that with HBr, the HBr molecule appears to donate electrons from the bromine atom to the carbon atom of the CO_2 molecule. This change in the EDA natures of the interacting species from HF and HCl to HBr has been interpreted [14] as being due to the competition between the higher acidities of HF and HCl favouring the linear hydrogen-bonded structure, and the higher energy of the dispersive interaction in the HBr complex relative to those with HF and HCl which would favour the T-shaped geometry. In the case of the complex formed between BF_3 and CO_2, the major alternative structures appear to be a linear B···OCO bonded symmetric top species, similar to the FH·OCO and ClH·OCO complexes, and a non-linear B···O bonded asymmetric top structure. The structure of $BF_3{\cdot}CO_2$ in the gas phase has been reported briefly in a study of $BF_3{\cdot}NCCN$, among other complexes, by Leopold et al. [106], who concluded that $BF_3{\cdot}CO_2$ was an asymmetric rotor, consistent with a non-linear B···OCO arrangement, as suggested by a lone pair-directed interaction, according to the structural rules applying to hydrogen-bonded complexes proposed by Legon and Millen [107]. In this paper we report the results of our ab initio studies on three possible B···O bonded isomers of the 1:1 $BF_3{\cdot}CO_2$ complex.

2 Computational methodology

The calculations were performed using the GAUSSIAN-92 computer program [108], at the second-order level of Møller-Plesset perturbation theory (MP2) [109], and with the 6-31G* split-valence polarized basis set [110]. Full geometry optimizations were carried out using the VERYTIGHT convergence criterion, with all molecular orbitals included in the post-self-consistent field (SCF) steps, subject to the imposition of C_S or C_{3V} symmetry, as appropriate. The interaction energies were computed by subtracting the sum of the energies of the monomers in their distorted geometries, as found in the complexes, from the energy of the complex in each case. These complexation energies were then corrected for basis set superposition error (BSSE) [111] by the Boys-Bernardi full counterpoise technique [112]. The total interaction energies were separated into the dispersion and the SCF contributions by subtraction of the computed Hartree-Fock energies from the MP2 energies, and the SCF parts of the interaction energies were decomposed into their electrostatic, polarization, charge transfer and exchange repulsion components using the Morokuma partitioning procedure [113, 114] as implemented in the MONSTERGAUSS program [115]. The total MP2 electronic energies were algebraically combined with the thermal energy differences, including the zero-point energy differences, and the pressure-volume energy terms to yield the enthalpy changes, as proposed by Del Bene [116].

Wavenumbers, infrared intensities and normal modes of vibration were computed using the FREQ option of GAUSSIAN-92 [108]. The normal coordinate analysis of the most favourable structure was performed with Shell and Steele's vibrational analysis program VIBRA [117].

3 Results and discussion

3.1 Geometries

The computed bond lengths, at the MP2 level, of the BF_3 and CO_2 monomers are 132.36 and 117.97 pm respectively. These values were obtained by fixing the bond angles at 120° and 180° respectively, and they compare with the experimental gas-phase values of 131.33 pm [118] and 116.0 pm [119] respectively, indicating overestimation of the bond lengths by 0.78 and 1.70% respectively. Three plausible structures were considered for the $BF_3{\cdot}CO_2$ complex, two of C_S and one of C_{3V} symmetry. In one of these structures (I), one of the oxygen atoms is bonded to the boron, with the OCO molecule eclipsing the BF bond lying in the symmetry plane (Fig. 1a). In the second (II), the interaction is again of the B···O type, but the OCO subunit is staggered with respect to the BF bonds (Fig. 1b). The third structure (III), shown in Fig. 1c, features a linear B···OCO fragment and was constrained to have C_{3V} symmetry. The computed geometrical parameters of these three structures are collected in Table 1, while Table 2 indicates the differences between the complex parameter values and those of the corresponding monomers. The conformations of structures I and II influence the bond lengths of the BF_3 molecule quite substantially; in the eclipsed case the in-plane BF bond is stretched significantly while the other two BF bonds remain virtually unchanged, and in the staggered

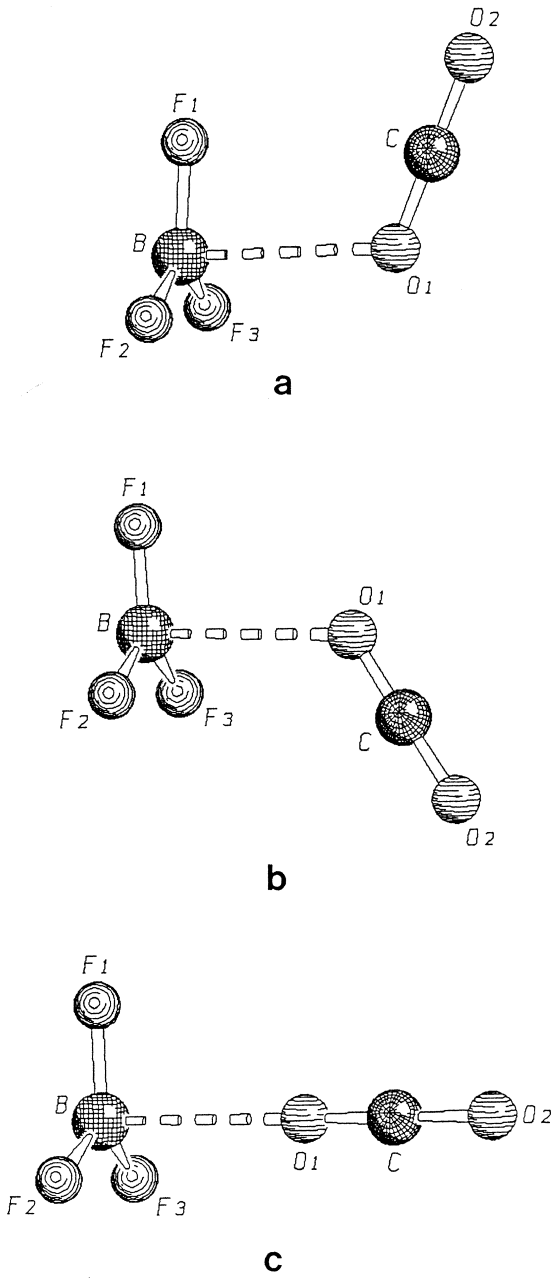

Fig. 1a–c. Optimized structures of three complexes of boron trifluoride and carbon dioxide: **a** eclipsed (I), **b** staggered (II) **c** linear (III)

Table 1. Optimized geometrical parameters (MP2/6-31G*) of some boron trifluoride-carbon dioxide complexes

Parameter	Complex		
	I (eclipsed)	II (staggered)	III (linear)
r(BF1)/pm	132.97	132.27	132.46
r(BF2)/pm	132.29	132.61	132.46
r(BF3)/pm	132.29	132.61	132.46
r(CO1)/pm	118.26	118.21	117.99
r(CO2)/pm	117.64	117.67	117.71
r(B···O1)/pm	262.29	259.71	260.81
F1$\hat{B}$F2/deg	119.75	120.19	119.98
F1$\hat{B}$F3/deg	119.75	120.19	119.98
F2$\hat{B}$F3/deg	120.43	119.55	119.98
O1$\hat{C}$O2/deg	179.47	179.48	[c]
F1$\hat{B}$···O1/deg	85.38	94.31	90.88
F2$\hat{B}$···O1/deg	93.68	89.24	90.88
F3$\hat{B}$···O1/deg	93.68	89.24	90.88
B···$\hat{O}$1C/deg	114.33	123.03	[c]
F1$\hat{B}$···O1C[a]/deg	0.0[b]	180.0[b]	[c]
F2$\hat{B}$···O1C[a]/deg	119.58	120.22	[c]
F3$\hat{B}$···O1C[a]/deg	119.58	120.22	[c]
B···$\hat{O}$1CO2[a]/deg	180.0	180.0	[c]

[a] Dihedral angle
[b] Fixed
[c] B···O1CO2 fragment fixed to be linear

Table 2. Computed complex-monomer differences in the geometrical parameters (MP2/6-31G*) of some boron trifluoride-carbon dioxide complexes

Parameter	Complex		
	I (eclipsed)	II (staggered)	III (linear)
r(BF1)/pm	0.61	−0.09	0.10
r(BF2)/pm	−0.07	0.25	0.10
r(BF3)/pm	−0.07	0.25	0.10
r(CO1)/pm	0.29	0.24	0.02
r(CO2)/pm	−0.33	−0.30	−0.26
F1$\hat{B}$F2/deg	−0.25	0.19	−0.02
F1$\hat{B}$F3/deg	−0.25	0.19	−0.02
F2$\hat{B}$F3/deg	0.43	−0.45	−0.02
O1$\hat{C}$O2/deg	−0.53	−0.52	0.0

complex the in-plane bond length changes very little, but the two equivalent BF bond lengths increase markedly. These structural observations may be rationalized by proposing that the eclipsed conformer is stabilized by an electrostatic attraction of the negatively charged in-plane fluorine atom for the positively charged carbon atom, separated by a distance of 301.3 pm. In the staggered conformer the carbon is separated by 343.7 pm from the two closer fluorines, and the combination of the larger distance of separation and the less favourable mutual orientation of the orbitals reduces the strength of the attractive interaction. In the linear species, the carbon lies at a distance of 403.2 pm from the three equivalent fluorines, and the attractive interaction is partially shielded by the intervening oxygen atom, O1 (Fig. 1c). The CO bond lengths of the CO_2 fragment change in the same way and by about the same amount, regardless of the conformation, the bonded CO bond stretching and the non-bonded CO bond length decreasing. Similarly, the signs of the changes in the values of the FBF bond angles are opposite in the eclipsed and the staggered cases. In the former the angle between the two equivalent BF bonds opens out while in the latter it closes up; the approximate planarity of the BF_3 unit is maintained in each case. For both structures I and II the OCO molecule retains its linearity within 1°. The changes in the parameters of the linear isomer on complexation are less pronounced. The BF bond lengths increase slightly while the free CO bond shortens by about the same amount as in structures I and II.

3.2 Energetics

Table 3 shows the absolute energies at both the restricted Hartree-Fock (RHF) and the MP2 levels, and the MP2 dipole moments. At the MP2 level the sequence of energies is eclipsed < staggered < linear, while the dipole moments follow the opposite trend. The trend in the energies is in accord with that in the bond lengths discussed above. Since neither monomer molecule possesses a permanent dipole moment in its equilibrium structure, the induction of the dipole moments in the complexes is related to the extent of perturbation of the monomer structures. In the linear complex the larger dipole moment enhancement is chiefly associated with the relatively large compression of the non-bonded CO bond, while in structures I and II the enhancements are due to a combination of several structural changes.

Table 3. Absolute energies and dipole moments of some boron trifluoride-carbon dioxide complexes

Complex	Energy/a.u.		Dipole moment/D[a]
	(RHF)[b]	(MP2)	(MP2)
Eclipsed	−510.825355028	−511.89205763978	0.4618
Staggered	−510.825288776	−511.89165126811	0.5507
Linear	−510.825477311	−511.89136706833	0.6304

[a] 1 D ≡ 3.336×10^{-3} Cm
[b] Restricted Hartree-Fock

The interaction energies, uncorrected and corrected for BSSE [111], are collected together in Table 4. It is found that the BSSE correction represents a substantial fraction of the total interaction energy for all three structures. The magnitude of the BSSE correction is proportional to the uncorrected stabilization energy, with the result that after correction the sequence of binding energies becomes linear > staggered > eclipsed, the opposite trend to that of the absolute energies. The trend in the values of the BSSE corrections is related to the extent to which the orbitals of the monomer units perturb one another, so that the largest BSSE correction is found in the complex in which the energetic stabilization is greatest. After separating out the dispersion energy of each conformer, the remaining SCF energy was partitioned into its respective components, as shown in Table 5. Of the attractive contributions the electrostatic part was found to predominate, followed by the charge transfer and polarization terms, in that order. The exchange repulsion term approximately balances the electrostatic attraction in each case. The corrected electronic interaction energies of Table 4 were further corrected for the differences in thermal and zero-point energies, and the pressure-volume energy differences, in order to reduce the electronic energy changes on complexation to enthalpy changes [116]. These are shown in Table 6. While all three complex structures are predicted to be stable relative to the separated monomers, the enthalpies of interaction follow the trend linear > staggered > eclipsed.

3.3 Mulliken charges

The Mulliken atomic charges [120] are presented in Table 7. This table also indicates the changes in the charges on each atom resulting from complexation, and the amount of charge transferred from donor to acceptor. While CO_2 is invariably the electron donor, as expected, the amount of charge transferred is always less than 10 me. The effect of the charge redistribution is that the three fluorine atoms, but especially the ones closer to the CO_2 molecule, gain charge, as does the bonded oxygen atom, at the expense of the boron and carbon, and the non-bonded oxygen atoms. The individual atoms which suffer the largest charge perturbations are, not unexpectedly, those most intimately involved in the EDA interaction, B and O1 (Fig. 1a–c).

Table 4. Interaction energies (MP2/6-31G*) of some boron trifluoride-carbon dioxide complexes

Complex	Energy/kJ mol^{-1}		
	Uncorrected	BSSE[a]	Corrected
Eclipsed	−15.406	10.854	−4.552
Staggered	−14.275	9.449	−4.826
Linear	−13.394	7.631	−5.763

[a] Basis set superposition error

3.4 Vibrational spectrum

Tables 8, A-2 [*g*] and A-3 [*g*] list the computed wavenumbers and infrared band intensities of the two C_S complexes (I and II) and the C_{3V} structure (III). The approximate descriptions of the intramolecular normal modes follow those of the corresponding monomer vibrations, while the intermolecular modes are described as B···O stretching, and libration of the CO_2 and BF_3 monomer units, either in-plane or out-of-plane. The values of the corresponding wavenumbers of all three species are fairly similar, the obvious exception being the calculation of a negative eigenvalue for the out-of-plane libration of the CO_2 unit in the staggered species II, and a similar negative eigenvalue for the doubly degenerate counterpart in the linear structure III. This mode is the one responsible for the conversion of structures II and III to structure I, and identifies II as a first-order and III as a second-order transition state on the potential energy surface, connecting two equivalent eclipsed structures separated by dihedral angles of 360°. As was the case with the wavenumbers, relatively small differences are observed between the intensities of corresponding modes in all three structures.

The computed wavenumber shifts and changes in the infrared intensities of the monomer bands accompanying association are shown in Table 9, for structure I, and

Table 5. BSSE-corrected Morokuma decompositions of the MP2/6-31G* interaction energies of some boron trifluoride-carbon dioxide complexes

Component	Energy/kJ mol^{-1}		
	Eclipsed	Staggered	Linear
Dispersion	−0.491	−0.346	−0.309
Electrostatic	−14.731	−14.832	−13.346
Charge transfer	−5.395	−4.714	−3.348
Polarization	−2.290	−2.299	−2.018
Exchange	15.314	14.511	11.131
Mixing	3.041	2.854	2.127
Total	−4.552	−4.826	−5.763

Table 6. Interaction enthalpies (MP2/6-31G*) of some boron trifluoride-carbon dioxide complexes

Complex	Energy/kJ mol^{-1}			
	ΔE(electronic)	ΔE(thermal)	Δ(pV)	ΔH
Eclipsed	−4.552	6.123	−2.479	−0.908
Staggered	−4.826	3.642	−2.479	−3.663
Linear	−5.763	1.232	−2.479	−7.010

Table 7. Mulliken atomic charges (MP2/6-31G*) of the boron trifluoride and carbon dioxide monomers and of some of their complexes, and their changes on complexation

Complex	Atom	Charge/e			
		Complex	Monomer	Difference	Fragment
Eclipsed	B	1.0156	0.9852	0.0304	
	F1	−0.3535	−0.3284	−0.0251	
	F2, F3	−0.3338	−0.3284	−0.0054	
					−0.0055
	C	0.9400	0.9186	0.0214	
	O1	−0.4932	−0.4593	−0.0339	
	O2	−0.4413	−0.4593	0.0180	
					0.0055
Staggered	B	1.0186	0.9852	0.0334	
	F1	−0.3341	−0.3284	−0.0057	
	F2, F3	−0.3461	−0.3284	−0.0177	
					−0.0077
	C	0.9400	0.9186	0.0214	
	O1	−0.4907	−0.4593	−0.0314	
	O2	−0.4416	−0.4593	0.0177	
					0.0077
Linear	B	1.0184	0.9852	0.0332	
	F1, F2, F3	−0.3417	−0.3284	−0.0133	
					−0.0067
	C	0.9367	0.9186	0.0181	
	O1	−0.4856	−0.4593	−0.0263	
	O2	−0.4446	−0.4593	0.0147	
					0.0065

Table 8. Computed wavenumbers and infrared intensities (MP2/6-31G*) of the eclipsed boron trifluride-carbon dioxide complex

Symmetry species	Mode	Approximate description	Wavenumber/ cm^{-1}	Intensity/ km mol^{-1}
a′	ν_1	$\nu_a(CO_2)$	2447	500.7
	ν_2	$\nu_a(BF_3)$	1477	379.5
	ν_3	$\nu_s(CO_2)$	1334	1.67
	ν_4	$\nu_s(BF_3)$	883	0.73
	ν_5	$\delta_s(BF_3)$	673	170.9
	ν_6	$\delta(CO_2)$	640	30.4
	ν_7	$\delta_a(BF_3)$	481	11.6
	ν_8	$l(BF_3)$	140	0.75
	ν_9	ν(B···O)	78	0.88
	ν_{10}	$l(CO_2)$	43	0.35
a″	ν_{11}	$\nu_a(BF_3)$	1502	390.5
	ν_{12}	$\gamma(CO_2)$	633	24.3
	ν_{13}	$\delta_a(BF_3)$	481	11.3
	ν_{14}	$l(BF_3)$	73	0.009
	ν_{15}	$l(CO_2)$	21	0.0002

Table 9. Computed complex-monomer wavenumber shifts and infrared intensity ratios (MP2/6-31G*) of the eclipsed boron trifluoride-carbon dioxide complex

Monomer	Mode		Wavenumber shift/ cm^{-1}	Intensity ratio[a]
BF_3	$\nu_s(BF_3)$		−6	–[b]
	$\delta_s(BF_3)$		−26	1.70
	$\nu_a(BF_3)$	(a′)	−20	0.93
		(a″)	5	0.95
	$\delta_a(BF_3)$	(a′)	0	0.91
		(a″)	0	0.88
CO_2	$\nu_s(CO_2)$		1	–[b]
	$\delta(CO_2)$	(a′)	4	1.19
		(a″)	−3	0.95
	$\nu_a(CO_2)$		−1	1.11

[a] Ratio = complex/monomer intensity
[b] Monomer mode is infrared inactive

Table 10. Definitions of the internal coordinates of the eclipsed boron trifluoride-carbon dioxide complex

Internal cordinate	Definition[a]
t_1	r(CO1)
t_2	r(CO2)
d	r(BF1)
r_1	r(BF2)
r_2	r(BF3)
R	r(B···O1)
α	F2$\hat{B}$F3
β_1	F1$\hat{B}$F2
β_2	F1$\hat{B}$F3
γ	F1$\hat{B}$···O1
δ_1	F2$\hat{B}$···O1
δ_2	F3$\hat{B}$···O1
ε	B···$\hat{O}$1C
θ	O1$\hat{C}$O2[b]
ϕ	O1$\hat{C}$O2[c]
τ	F1B···O1C[d]

[a] See Fig. 1a for the structure of the eclipsed complex
[b] In the symmetry plane
[c] Perpendicular to the symmetry plane
[d] Torsional angle

Table 11. Definitions of the symmetry coordinates of the eclipsed boron trifluoride-carbon dioxide complex

Symmetry species	Symmetry coordinate	Definition
a′	S_1	$(\Delta t_1 - \Delta t_2)/2^{-1/2}$
	S_2	$(2\Delta d - \Delta r_1 - \Delta r_2)/6^{-1/2}$
	S_3	$(\Delta t_1 + \Delta t_2)/2^{-1/2}$
	S_4	$(\Delta r_1 + \Delta r_2)/2^{-1/2}$
	S_5	$(\Delta\gamma + \Delta\delta_1 + \Delta\delta_2 - \Delta\alpha - \Delta\beta_1 - \Delta\beta_2)/6^{-1/2}$
	S_6	$\Delta\theta$
	S_7	$(2\Delta\alpha - \Delta\beta_1 - \Delta\beta_2)/6^{-1/2}$
	S_8	$(2\Delta\gamma - \Delta\delta_1 - \Delta\delta_2)/6^{-1/2}$
	S_9	ΔR
	S_{10}	$\Delta\varepsilon$
a″	S_{11}	$(\Delta r_1 - \Delta r_2)/2^{-1/2}$
	S_{12}	$\Delta\phi$
	S_{13}	$(\Delta\beta_1 - \Delta\beta_2)/2^{-1/2}$
	S_{14}	$(\Delta\delta_1 - \Delta\delta_2)/2^{-1/2}$
	S_{15}	$\Delta\tau$

in Tables A–4 [*g*], and A–5 [*g*] for the other isomers. The complex-monomer wavenumber differences are all less than 30 cm^{-1}, while the intensity ratios lie in a rather narrow band of values, from 0.88 to 1.85. The observation of small wavenumber shifts, and intensity ratios of the complex bands close to unity, testifies to the fact that the perturbations of each monomer spectrum by interaction with the partner monomer are minimal.

In the light of the fact that structure I was the only one for which the vibrational analysis yielded no negative eigenvalues, we have extended that analysis, using the VIBRA program [117], in order to determine the vibrational force field of this species.

3.5 Vibrational force field

The internal coordinates employed in the normal mode analysis are defined in Table 10, in terms of the geometrical parameters identified in Fig. 1a. The vibrational modes transform as

$$\Gamma_{vib} = 10a' + 5a''$$

under C_S symmetry (see Table 8), and a suitable set of symmetry coordinates is shown in Table 11. Table 12 reports the percentage potential energy distributions (PEDs) of each normal mode among the symmetry coordinates, for the a′ and a″ species vibrations.

The PEDs of the a′ species confirm the accuracy of the descriptions of the intramolecular modes given in Table 8, indicating particularly that the CO_2 stretching vibrations are localized solely in the CO bonds (see Table 12). For the BF_3 stretching motions the higher frequency mode is a coupling of the two symmetry coordinates describing the a′ antisymmetric vibrations, while the lower of the two is restricted, exclusively, to the two out-of-plane BF bonds. The two BF_3 bending and the CO_2 bending vibrations are concentrated over 90% in symmetry coordinates S_5, S_6 and S_7. The intermolecular modes, however, show a high degree of coupling of the CO_2 bending, the BF_3 libration, the B···O stretching and the B···OC bending (140 cm^{-1}), the BF_3 libration and the B···O stretching (78 cm^{-1}) and the CO_2 bending and the B···OC bending vibrations (43 cm^{-1}). Table 12 shows that the antisymmetric BF_3 stretching vibration contains a contribution of over 10% of the antisymmetric bending motion, and the remaining a″ intramolecular modes are very highly localized in symmetry coordinates S_{12} and S_{13}. The 73 cm^{-1} vibration is largely the libration of the BF_3 moiety about the in-plane BF bond, while the lowest frequency mode is mainly the torsion about the B···O bond, but with a significant component due to the out-of-plane CO_2 bending.

The intermolecular valence force constants of the complex, the intermonomer stretching and the in-plane and out-of-plane intermonomer bending force constants, are presented in Table 13, which also includes a comparison of the complex force constants with the corresponding values for the monomers. The value of the B···O stretching force constant, 13.94 Nm^{-1}, appears to be typical for an intermolecular vibration of a weakly bonded aggregate, and the systematic decrease in magnitude from the stretching to the in-plane bending (6.66 Nm^{-1}) to the out-of-plane bending (0.85 Nm^{-1}) is also a characteristic feature of the spectra of molecular complexes. The remaining major force constants of the complex indicate that the greatest perturbations are the decreases of the in-plane BF stretching and the out-of-plane FB···O bending constants of the BF_3 moiety and the bonded CO stretching and the out-of-plane OCO bending of the CO_2 fragment. There is also a noticeable increase in the stretching force constant of the non-bonded CO bond, relative to that of the CO_2 monomer.

3.6 Prediction of experimental infrared spectrum

The experimental spectrum of species I should show 15 fundamental vibration bands (see Table 8). Of these, all

Table 12. Percentage potential energy distributions of the normal modes of the eclipsed boron trifluoride-carbon dioxide complex

Wavenumber/cm^{-1}	a′ Symmetry									
	Symmetry coordinate									
	S_1	S_2	S_3	S_4	S_5	S_6	S_7	S_8	S_9	S_{10}
2447	100.0									
1477		67.4		27.2			5.4			
1334			100.0							
883				100.0						
673					96.5				3.5	
640						90.3				9.7
481		6.1		2.0			91.8			
140					1.0	24.9		14.4	24.4	35.3
78					1.1		0.5	44.6	53.8	
43		0.1				44.6		0.9	0.6	53.7

Wavenumber/cm^{-1}	a″ Symmetry				
	Symmetry coordinate				
	S_{11}	S_{12}	S_{13}	S_{14}	S_{15}
1502	88.5		11.5		
633		99.1			0.9
481	3.3		96.7		
73		3.0	2.0	90.1	5.0
21		29.0	0.3	4.5	66.2

Table 13. Major valence force constants of the eclipsed boron trifluoride-carbon dioxide complex, and differences between complex and monomer force constants

Force constant[a]	Force constant/Nm^{-1}				
	Complex	BF_3 monomer	Difference[b]	CO_2 monomer	Difference[b]
f_R	13.94				
f_ε	6.66				
f_τ	0.85				
f_d	734.09	762.55	−28.46		
f_r	762.28	762.55	−0.27		
f_γ	72.43	79.00	−6.57		
f_δ	58.72	79.00	−20.28		
f_{dr}	60.45	60.98	−0.53		
f_{rr}	60.48	60.98	−0.50		
f_{t1}	1588.85			1617.38	−28.54
f_{t2}	1633.00			1617.38	15.61
f_θ	186.75			189.38	−2.63
f_ϕ	123.49			189.38	−65.89
f_{tt}	68.58			67.23	1.35

[a] See Table 10 and Fig. 1a for definitions of internal coordinates
[b] Difference = complex − monomer force constant

the intermolecular modes are expected to absorb below about 150 cm^{-1}, and are in any case very weak; hence the probability of observing them experimentally is rather low.

In the BF_3 monomer regions of the complex spectrum, the symmetric BF_3 stretching mode is calculated to be displaced by 6 cm^{-1} to the low frequency of the monomer position, but since the monomer mode is infrared inactive and the complex mode is predicted to have a very low intensity, the complex absorption band is unlikely to be readily observed. The out-of-plane BF_3 bending mode is computed to shift by 26 cm^{-1} to the low frequency of the monomer band, the largest predicted shift in the spectra of any of the three species. The relatively high calculated intensity militates in favour of this mode being a good diagnostic feature. The degenerate monomer antisymmetric stretching mode splits into a pair of vibrations, one 20 cm^{-1} to the red and the other 5 cm^{-1} to the blue of the monomer. The antisymmetric BF_3 bending mode is insensitive to complexation, the predicted shifts being zero for both the a′ and a″ components.

Among the modes derived from the CO_2 monomer, the symmetric CO_2 stretching is predicted to show a very small shift from the monomer value, and to be very weak. Since the corresponding monomer mode is infrared inactive, however, it would not be observed in an experimental spectrum and therefore would not provide a marker from which to measure the complex shifts. This mode is therefore of little value in identifying the complex in a matrix isolation spectrum. The antisymmetric CO_2 stretching mode of the complex shows virtually no displacement from the monomer band. Thus, although this mode is predicted to give rise to the strongest band in the spectrum, its utility in identifying the complex in a matrix is also limited. The CO_2 bending vibration holds more promise for diagnostic purposes, since it is split into two modes, which shift in opposite directions with respect to the monomer absorption. These shifts are very small (4 and −3 cm^{-1}), but the predicted intensities are of intermediate magnitude.

Thus the most useful vibrational features for characterizing the complex are the antisymmetric BF_3 stretching, the symmetric BF_3 bending and the CO_2 bending modes, where the lifting of the degeneracies of the first and third of these vibrations yield one band shifted to either side of the monomer absorption, while the symmetric BF_3 bending suffers a substantial red shift.

A recent high resolution microwave study of four isotopomers of BF_3. CO_2 [121] has been interpreted in terms of a symmetric top with a large amplitude motion and an anomalously large value of D_{JK}. The vibrationally averaged monomer centre-of-mass separation was determined to be 376 pm, which compares with the B···C distance determined here of 329.2 pm. This experimental observation is not necessarily in conflict with the theoretical conclusion presented here, however, and is open to the interpretation that the observed structure results from large amplitude motion about an asymmetric equilibrium structure, i.e. the complex is a quasi-symmetric top. It should also be recognized that the search for the existence of the complex in cryogenic matrices will not necessarily yield the same structure as that observed in the gas phase, partly because of the different time scales of the respective experiments, and partly because the large amplitude motion responsible for interconverting structures I, II and III may be quenched in the matrix, due to the influence of the matrix cage, but not in the gas phase.

Acknowledgements. T.A.F. acknowledges financial support from the Foundation for Research Development and the University of Natal Research Fund and G.A.Y. from the School of Chemistry, Technikon Witwatersrand, and L.M.N. thanks Sasol (Pty.) Ltd. for the award of a Postgraduate Research Bursary. The authors would also like to thank a referee for bringing the existence of reference 121 to their attention.

References

1. Evans DG, Yeo GA, Ford TA (1988) Faraday Discuss Chem Soc 86:55
2. Nxumalo LM, Ford TA (1996) J Mol Struct (Theochem) 369:115
3. Nxumalo LM, Andrzejak M, Ford TA (1996) J Chem Inf Comput Sci 36:377
4. Nxumalo LM, Andrzejak M, Ford TA (1996) Vib Spectrosc 12:221
5. Ford TA, Steele D (1996) J Phys Chem 100:19336
6. Nxumalo LM, Ford TA (1993) J Mol Struct 300:325
7. Nxumalo LM, Ford TA (1995) S Afr J Chem 48:30
8. Nxumalo LM, (1992) PhD thesis, University of the Witwatersrand, Johannesburg
9. http://link.springer.de/journals/tca/
10. Baiocchi FA, Dixon TA, Joyner CH, Klemperer W (1981) J Chem Phys 74:6544
11. Shea JA, Read WG, Campbell EJ (1983) J Chem Phys 79:614
12. Lovejoy CM, Schuder MD, Nesbitt DJ (1987) J Chem Phys 86:5337
13. Fraser GT, Pine AS, Suenram RD, Dayton DC, Miller RE (1989) J Chem Phys 90:1330
14. Sharpe SW, Zeng YP, Wittig C, Beaudet RA (1990) J Chem Phys 92:943
15. Nesbitt DJ, Lovejoy CM (1990) J Chem Phys 93:7716
16. Nesbitt DJ, Lovejoy CM (1992) J Chem Phys 96:5712
17. Altman RS, Marshall MD, Klemperer W (1982) J Chem Phys 77:4344
18. Klots TD, Ruoff RS, Gutowsky HS (1989) J Chem Phys 90:4216
19. Dayton DC, Pedersen LG, Miller RE (1990) J Chem Phys 93:4560
20. Weida MJ, Sperhac JM, Nesbitt DJ, Hutson JM (1994) J Chem Phys 101:8351
21. Randall RW, Walsh MA, Howard BJ (1988) Faraday Discuss Chem Soc 85:13
22. Fraser GT, Pine AS, Suenram RD (1988) J Chem Phys 88:6157
23. Pine AS, Fraser GT (1988) J Chem Phys 89:100
24. Iida M, Ohshima Y, Endo Y (1993) J Phys Chem 97:357
25. Steed JM, Dixon TA, Klemperer W (1979) J Chem Phys 70:4095
26. Hough AM, Howard BJ (1987) J Chem Soc Faraday Trans II 83:173, 191
27. Sharpe SW, Sheeks R, Wittig C, Beaudet RA (1990) Chem Phys Lett 151:267
28. Sharpe SW, Reifschneider D, Wittig C, Beaudet RA (1991) J Chem Phys 94:233
29. Mäder H, Heineking N, Stahl W, Jäger W, Xu Y (1996) J Chem Soc Faraday Trans 92:901
30. Iida M, Ohshima Y, Endo Y (1991) J Chem Phys 95:4772
31. Walsh MA, Dyke TR, Howard BJ (1988) J Mol Struct 189:111
32. Rice JK, Lovas FJ, Fraser GT, Suenram RD (1995) J Chem Phys 103:3877
33. Zeng YP, Sharpe SW, Shin SK, Wittig C, Beaudet RA (1992) J Chem Phys 97:5392
34. Legon AC, Suckley AP (1989) J Chem Phys 91:4440
35. Randall RW, Summersgill JPL, Howard BJ (1990) J Chem Soc Faraday Trans 86:1943
36. Leopold KR, Fraser GT, Klemperer W (1984) J Chem Phys 80:1039
37. Legon AC, Suckley AP (1989) Chem Phys Lett 157:5
38. Mannik L, Stryland JC, Welsh HL (1971) Can J Phys 49:3056
39. Novick SE, Davies PB, Dyke TR, Klemperer W (1973) J Am Chem Soc 95:8547
40. Lobue JM, Rice JK, Novick SE (1984) Chem Phys Lett 112:376
41. Peterson KI, Klemperer W (1984) J Chem Phys 80:2439
42. Block PA, Marshall MD, Pedersen LG, Miller RE (1992) J Chem Phys 96:7321
43. Rice JK, Coudert LH, Matsumura K, Suenram RD, Lovas FJ, Stahl W, Pauley DJ, Kukolich SG (1990) J Chem Phys 92:6408
44. Fraser GT, Leopold KR, Klemperer W (1984) J Chem Phys 81:2577
45. Fraser GT, Nelson DD, Charo A, Klemperer W (1985) J Chem Phys 82:2535
46. Barton AE, Chablo A, Howard BJ (1979) Chem Phys Lett 60:414
47. Pubanz GA, Maroncelli M, Nibler JW (1985) Chem Phys Lett 120:313
48. Jucks KW, Huang ZS, Dayton D, Miller RE, Lafferty WJ (1987) J Chem Phys 86:4341
49. Walsh MA, England TH, Dyke TR, Howard BJ (1987) Chem Phys Lett 142:265
50. Jucks KW, Huang ZS, Miller RE, Fraser GT, Pine AS, Lafferty WJ (1988) J Chem Phys 88:2185
51. Novick SE, Suenram RD, Lovas FJ (1988) J Chem Phys 88:687
52. Prichard DG, Nandi RN, Muenter JS, Howard BJ (1988) J Chem Phys 89:1245
53. Muenter JS (1989) J Chem Phys 90:4048
54. Huang ZS, Miller RE (1989) Chem Phys 132:185
55. Blake TA, Novick SE, Lovas FJ, Suenram RD (1992) J Mol Spectrosc 154:72
56. Bemish RJ, Block PA, Pedersen LG, Miller RE (1995) J Chem Phys 103:7788
57. Andrews L, Johnson GL (1982) J Chem Phys 76:2875

58. Andrews L (1984) J Phys Chem 88:2940
59. Andrews L, Arlinghaus RT, Johnson GL (1983) J Chem Phys 78:6353
60. Fourati N, Silvi B, Perchard JP (1984) J Chem Phys 81:4737
61. Raducu V, Jasmin D, Dahoo R, Brosset P, Gauthier-Roy B, Abouaf-Marguin L (1995) J Chem Phys 102:9235
62. Fredin L, Nelander B, Ribbegard G (1975) Chem Scr 7:11
63. Fredin L, Nelander B (1976) Chem Phys 15:473
64. van der Zwet GP, Allamandola LJ, Baas F, Greenberg JM (1989) J Mol Struct 195:213
65. Fredin L, Nelander B, Ribbegard G (1974) J Mol Spectrosc 53:410
66. Guasti R, Schettino V, Brigot N (1978) Chem Phys 34:391
67. Irvine MJ, Pullin ADE (1982) Aust J Chem 35:1961
68. Nxumalo LM, Ford TA (1994) J Mol Struct 327:145
69. Knözinger E, Beichert P (1995) J Phys Chem 99:4906
70. Le Quere AM, Xu C, Manceron L (1991) J Phys Chem 95:3031
71. Kollman P (1977) J Am Chem Soc 99:4875
72. Hurst GJB, Fowler PW, Stone AJ, Buckingham AD (1986) Int J Quantum Chem 29:1223
73. Alberts IL, Handy NC, Simandiras ED (1988) Theor Chim Acta 74:415
74. Sadlej J, Roos BO (1989) Theor Chim Acta 76:173
75. Muenter JS (1995) J Chem Phys 103:1263
76. Silvi B, Allavena M (1986) J Mol Struct (Theochem) 135:225
77. de Almeida WB (1990) Chem Phys Lett 166:589
78. Slanina Z, de Almeida WB (1991) J Mol Struct (Theochem) 235:51
79. Jönsson B, Karlström G, Wennerström H (1975) Chem Phys Lett 30:58
80. Nguyen MT, Ha TK (1984) J Am Chem Soc 106:599
81. Damewood JR, Kumpf RA, Mühlbauer WCF (1989) J Phys Chem 93:7640
82. Sadlej J, Maruzek P (1995) J Mol Struct (Theochem) 337:129
83. de Almeida WB (1990) Chem Phys 141:297
84. Bone RGA, Handy NC (1990) Theor Chim Acta 78:133
85. Parker GA, Snow RL, Pack RT (1976) J Chem Phys 64:1668
86. Clary DC (1982) Chem Phys 65:247
87. Sadlej J (1990) J Mol Struct (Theochem) 209:231
88. Keil M, Rawluk LJ, Dingle TW (1992) J Chem Phys 96:6221
89. Preston RK, Pack RT (1977) J Chem Phys 66:2480
90. Roche CF, Ernesti A, Hutson JM, Dickinson AS (1996) J Chem Phys 104:2156
91. Marshall PJ, Szczesniak MM, Sadlej J, Chalasinski G, ter Horst MA, Jameson CJ (1996) J Chem Phys 104:6569
92. Glauser WA, Koszykowski ML (1991) J Phys Chem 95:8507
93. Cox AJ, Ford TA, Glasser L (1993) In:Structures and conformations of non-rigid molecules, Laane J, Dakkouri M, van der Veken B, Oberhammer H (eds). Kluwer, Dordrecht, pp 391–408
94. Abashkin Y, Mele F, Russo N, Toscano M (1994) Int J Quantum Chem 52:1011
95. Jönsson B, Nelander B (1977) Chem Phys 25:263
96. Amos RD, Handy NC, Knowles PJ, Rice JE, Stone AJ (1985) J Phys Chem 89:2186
97. Koide A, Kihara T (1974) Chem Phys 5:34
98. Brigot N, Odiot S, Walmsley SH, Whitten JL (1977) Chem Phys Lett 49:157
99. Brigot N, Odiot S, Walmsley SH (1982) Chem Phys Lett 88:543
100. Illies AJ, McKee MJ, Schlegel HB (1987) J Phys Chem 91:3489
101. Eggenberger R, Gerber S, Huber H (1991) Mol Phys 72:433
102. Eggenberger R, Gerber S, Huber H, Searles D (1991) Chem Phys Lett 183:223
103. Muenter JS (1991) J Chem Phys 94:2781
104. Slanina Z, Kim SJ, Fox K (1993) Vib Spectrosc 4:251
105. Nxumalo LM, Ford TA, Cox AJ (1994) J Mol Struct (Theochem) 307:153
106. Leopold KR, Fraser GT, Klemperer W (1984) J Am Chem Soc 106:897
107. Legon AC, Millen DJ (1987) Acc Chem Res 20:39
108. Frisch MJ, Trucks GW, Head-Gordon M, Gill PMW, Wong MW, Foresman JB, Johnson BG, Schlegel HB, Robb MA, Replogle ES, Gomperts R, Andres JL, Raghavachari K, Binkley JS, Gonzalez C, Martin RL, Fox DJ, DeFrees DJ, Baker J, Stewart JJP, Pople JA (1992) GAUSSIAN-92, revision E.1, Gaussian, Inc., Pittsburgh, Pa
109. Møller C, Plesset MS (1934) Phys Rev 46:618
110. Francl MM, Pietro WJ, Hehre WJ, Binkley JS, Gordon MS, DeFrees DJ, Pople JA (1982) J Chem Phys 77:3654
111. Liu B, McLean AD (1973) J Chem Phys 59:4557
112. Boys SF, Bernardi F (1970) Mol Phys 19:553
113. Morokuma K (1971) J Chem Phys 55:1236
114. Kitaura K, Morokuma K (1976) Int J Quantum Chem 10:325
115. Peterson MR, Poirier RA (1981) MONSTERGAUSS, University of Toronto, Toronto
116. Del Bene JE (1986) In:Liebman JF, Greenberg A (eds) Molecular structure and Energetics, vol 1. VCH, Deerfield Beach, F1a, pp 319–349
117. Shell RC, Steele D (1985) VIBRA, University of London, London
118. Kuchitsu K, Konaka S (1966) J Chem Phys 45:4342
119. Harmony MD, Laurie VW, Kuczkowski RL, Schwendeman RH, Ramsay DA, Lovas FJ, Lafferty WJ, Maki AG (1979) J Phys Chem Ref Data 8:619
120. Mulliken RS (1955) J Chem Phys 23:1833
121. Grushow A, Goodfriend A, Phillips JA, Canagaratna M, Leopold KR, Fraser GT, Klemperer W (1995) Abstract TB05, 50th Ohio State University International Symposium on Molecular Spectroscopy, Columbus, Ohio